EUROFUSION WPJET2-PR(16) 14815

A Garcia-Carrasco et al.

# Modification of diagnostic mirrors in current and next-step fusion devices

Preprint of Paper to be submitted for publication in
22nd International Conference on Plasma Surface Interactions
in Controlled Fusion Devices (22nd PSI)

This work has been carried out within the framework of the EUROfusion Consortium and has received funding from the Euratom research and training programme 2014-2018 under grant agreement No 633053. The views and opinions expressed herein do not necessarily reflect those of the European Commission.

# Modification of diagnostic mirrors in JET

A. Garcia-Carrasco[a], P. Petersson[a], M. Rubel[a], A. Widdowson[b], E. Fortuna[c], M. Brix[b], L. Marot[d], and JET Contributors*

*EUROfusion Consortium, JET, Culham Science Centre, OX14 3DB, Abingdon, UK*

*[a]Royal Institute of Technology (KTH), SE-10044 Stockholm, Sweden*

*[b]EUROfusion Consortium, JET, Culham Science Centre, Abingdon, OX14 3DB, UK*

*[c]Department of Materials Science, Warsaw University of Technology, 02-502 Warsaw, Poland*

*[d]Department of Physics, University of Basel, Association EURATOM-CRPP, Switzerland*

*See the Appendix of F. Romanelli et al., Proceedings of the 25th IAEA Fusion Energy Conference 2014, Saint Petersburg, Russia

alvarogc@kth.se

## Abstract

All optical diagnostics in next-step fusion devices will rely on metallic mirrors acting as plasma-facing components. This contribution provides a comprehensive account on the modification of diagnostic mirrors in JET with the ITER-Like Wall. Specimens from the First Mirror Test and the lithium-beam diagnostic have been studied by spectrophotometry, ion beam analysis and electron microscopy. Test mirrors made of molybdenum were retrieved from the main chamber wall and the divertor after exposure to the 2013-2014 experimental campaign. In the main chamber, only mirrors located at the entrance of the carrier lost reflectivity (Be deposition from the eroded limiters), while those located deeper in the carrier were only slightly affected. The performance of mirrors in the JET divertor was strongly degraded by deposition of beryllium, tungsten and other species. Mirrors from the lithium-beam diagnostic have been studied for the first time. Gold coatings were severely damaged by intense arcing. As a consequence, material mixing of the gold layer with the stainless steel substrate occurred. Total reflectivity dropped from over 90% to less than 60 %, i.e. to the level typical for stainless steel.

**PACS: 52.40 Hf**

***Keywords:*** *JET, First Mirror Test, diagnostic mirrors, erosion-deposition*

## 1. Introduction

In the next generation of fusion devices, optical diagnostics will rely on plasma-facing mirrors, known as first mirrors, to access plasma while maintaining neutron shielding. Optical stability of first mirrors will be essential to ensure reliability of diagnostics [1]. As plasma-facing components, first mirrors will undergo modification due to plasma-wall interaction (PWI) processes. Erosion by impinging particles will change roughness and chemical composition of material by co-implantation. Deposition of plasma impurities together with fuel species will lead to the formation of coating layers on the surface of mirrors. Both situations will result in the degradation of reflectivity. There is an ongoing research in fusion experiments to assess the performance of first mirrors and to elaborate solutions to prolong their lifetime. Some examples are the works at JET [2], TEXTOR [3], DIII-D [4], Tore Supra [5] and HL-2A [6]. Also, laboratory experiments on simulation of neutron-induced effects are carried out to assess the impact of transmutation, material damage and helium production on optical properties of mirrors [7, 8].

The aim of this contribution is to provide a comprehensive account on the modification of diagnostic mirrors by PWI processes in JET with the ITER-Like Wall (ILW) [9]. Two different types of mirrors have been studied: (i) specimens from the First Mirror Test (FMT) [10-12] and (ii) the lithium-beam diagnostic mirrors.

The FMT project is realised for ITER with the aim to determine plasma impact on the optical performance of diagnostic mirrors. The project started in 2001 on request of the ITER Design Team. The FMT research program involves: (i) selection of material for mirrors, (ii) production of mirrors and their carriers for in-vessel installation, (iii) optical pre-characterization, (iv) exposure in different locations in JET (main chamber and divertor) during a complete operational campaign, and (v) comprehensive post-mortem analyses by means of surface-sensitive techniques to assess optical properties and morphology. Until now, complete sets of results have been obtained after two experimental campaigns in JET-C, i.e. with carbon walls [10, 11] and after the first experimental campaign (2011-2012) in JET-ILW [12]. This work concentrates on mirrors exposed during the second ILW campaign in 2013-2014.

The purpose of the lithium-beam diagnostic system at JET is to measure electron density profiles at the plasma edge. It is based on the injection of a neutral lithium beam with energies of 20-70 kV and the subsequent analysis of photon-emission profiles produced by the

interaction of lithium with plasma electrons. Because a wide variety of plasma shapes are explored at JET, it is necessary to use a mirror with an adjustable tilt angle to detect light from a given region of interest at the plasma edge [13, 14]. It should be stressed that these are the first-ever surface studies on actual diagnostic mirror from JET.

## 2. Experimental

### *2.1 Mirrors*

Twenty test mirrors were retrieved from JET-ILW after the 2013-2014 experimental campaign. The total plasma exposure time was 70013 s, including limiter (21373 s) and divertor (48640 s) configurations, i.e. fairly similar to the operation time in the first ILW campaign in 20011-2012. All mirrors were made of polycrystalline molybdenum with a surface area of 1 x 1 $cm^2$. Some surfaces were additionally coated using magnetron sputtering with a 1 μm thick layer of molybdenum or rhodium. Test mirrors were installed in stainless steel carriers placed in the outer mid-plane of the main chamber wall and in the divertor: outer and inner leg and below the base tile. The carriers had channels in which mirrors could be mounted at different depths, thus having different solid angles with respect to plasma.

The Li-beam diagnostic mirrors were retrieved after the 2011-2012 and 2013-2014 experimental campaigns. The mirrors were 13 x 5 $cm^2$ and 1 cm thick plates made of bulk stainless steel with a gold coating. They were installed in a periscope head on top of the vessel at about 42 cm from plasma. Figure 1 shows the top of JET vessel with the Li-beam diagnostic mirror in the periscope head surrounded by various types of limiters, e.g. castellated mushroom roof limiters.

### *2.2. Analysis methods*

The most important property of a mirror is reflectivity. Relevant measurements were performed in a glove-box to comply with safety procedures for beryllium- and tritium-contaminated material from JET. The system to measure reflectivity was composed of: (i) a tungsten halogen lamp as a light source, (ii) a CCD spectrometer for the visible range, (iii) an InGaAs photodiode spectrometer for the near infra-red (NIR) range, (iv) an integrating sphere, 80 mm in diameter, with an optional aperture to measure either total or diffuse reflectivity. The light source and spectrometers were located outside the glove-box. Only the integrating sphere and the samples to be analysed were placed inside to have maximum operation space and also to reduce the cost of equipment.

Surface and near-surface composition of the exposed mirrors was examined using several complementary accelerator-based methods at the Tandem Accelerator Laboratory (Uppsala University, Sweden). Deuterium and beryllium concentrations were measured by nuclear reaction analysis (NRA) with a 2.8 MeV $^{3}He^{+}$ beam. This method cannot be used to measure carbon in beryllium contaminated samples because protons produced from the nuclear reactions $^{12}C(^{3}He, p)^{4}He$ and $^{9}Be(^{3}He,p)^{11}B$ have similar energies and the resulting energy spectrum cannot be resolved. Tungsten concentration was measured using Rutherford backscattering spectrometry (RBS), also with a 2.8 MeV $^{3}He^{+}$ beam. The thickness of the gold coating of the Li-beam diagnostic mirrors was measured by RBS using a 3 MeV proton beam. Concentration of light species (Be, C, N and O) was measured by time-of-flight heavy ion elastic recoil detection analysis (ToF-ERDA) with a 36 MeV $^{127}I^{8+}$ beam. This method is suited to determine composition depth profiles because of excellent mass separation between light elements and good depth resolution of a few nm [15]. The main disadvantage is the sensitivity to surface roughness because of low incidence angle (22°). However, this is not an issue in the analysis of mirrors.

The morphology and composition of mirror surfaces was studied also by means of optical and scanning electron microscopy (SEM) using Hitachi SU8000 (beam energy 0.5-30 keV) combined with energy-dispersive X-ray spectroscopy (EDS Thermo Scientific Ultra Dry, type SDD – silicon drift detector) and YAG BSE (backscattered electrons) detector. The EDS system is capable of beryllium detection and quantification, as shown earlier in studies of dust specimens from the JET divertor [16].

## 3. Results

### *3.1 First Mirror Test*

#### *3.1.1 Mirrors from the divertor*

Visual inspection revealed that all divertor mirrors were covered with smooth-looking layers displaying a variety of colourful patterns thus indicating inhomogeneous material deposition. The appearance of several surfaces is presented in Figure 2. The total reflectivity was degraded by 50 – 80 % regardless of the substrate material or the location in the carrier. Plots in Figure 3 show the reflectivity for the outer divertor mirrors before and after the exposure to plasma. The distances in the legend refer to the depth of the mirror in the channel of the

carrier. Diffuse reflectivity is below 5 % over the measured spectral range. It confirms that surface has remained fairly smooth despite the presence of co-deposits.

Surface composition of divertor mirrors is presented in Table 1. The main impurity is beryllium, followed by oxygen, nitrogen, deuterium, carbon, tungsten and traces of Inconel constituents (Ni, Cr, Fe); the latter is not shown in the table. The total thickness of deposits is in the range from 50 to 500 nm. Such layer thickness completely blocks the light from reaching the mirror substrate. This explains why reflectivity of all mirrors is degraded to a similar level regardless of the position and the substrate (Mo or Rh), because the reflected signal originates from the deposit itself.

Impurity concentrations are similar to those measured on the mirrors exposed to the 2011-2012 experimental campaign [12] with the exception of carbon, whose levels are significantly lower, nearly by a factor of 10. The reason is that during the 2011-2012 experimental campaign, mirrors were installed in-vessel right after changing from the carbon to the metal first wall. During the initial operation phase, carbon concentration in plasma was higher due to carbon residues [17]. An example of a concentration depth profile is shown in Figure 4. It is recorded for a rhodium-coated mirror from the inner divertor placed 1.5 cm into the channel of the carrier. Traces for only some impurity species (Be, O, C, N) are shown for clarity of the figure. The thickness of the deposit is approximately 100 nm. It is composed mainly of beryllium and oxygen. The increase of oxygen at a depth of 50 nm is most probably associated with the in-vessel intervention (and venting the torus) to retrieve a broken reciprocating probe. The measured fluctuation of the oxygen content in deposits reflects the machine operation history. One may tentatively state that the oxygen detected in the co-deposit is associated with in-vessel processes (co-deposition of O impurity species) and not with the oxidation of the entire layer once mirrors were removed from the torus.

*3.1.2 Mirrors from the main chamber wall*

The total reflectivity plots for the mirrors from the main chamber wall are shown in Figure 5. There is a decrease in reflectivity by about 20% for the specimen located at the entrance of the carrier. However, reflectivity of all other mirrors is maintained or even slightly increased in the visible range as a result of erosion of Mo oxides by impinging neutral particles, as discussed in more detail in [12]. Diffuse reflectivity has not changed significantly after plasma exposure: it is below 5% over the measured spectral range.

Surface composition of the mirrors is presented in Table 2. There is a significant difference between the specimen at the carrier entrance and those located deeper. In the latter case the concentrations of D, Be, C, N and O impurities are at the level of about 1-3x$10^{16}$ $cm^{-2}$, while tungsten is below the detection limit of 5x$10^{13}$ $cm^{-2}$. On the contrary, the mirror at the entrance (position 0 cm) is coated by a layer of 600 nm composed mainly of beryllium. Photographic survey performed during the shut-down showed melting of beryllium limiters in the vicinity of the mirror carrier. The fairly thick beryllium layer was most probably deposited on the mirror surface during such off-normal events.

Results of detailed topographical studies performed with SEM and EDS on the mirror at position 0 cm are shown in Figure 6 and 7. On top of the fairly uniform co-deposits there are numerous macroscopic particles of various shape and size: from 3 μm to over 100 μm. These are elongated splashes (Fig. 6 (a-d)), flat splashes (Fig.6 (e)) and spherical droplets (Fig. 7(a)). The variety of objects gives strong indication that they were deposited at different events. The elongation proves that splashing occurred under strong magnetic field. The splashes cannot be associated with a single disruption because they have different orientations. A common feature of all these objects is the presence of beryllium as the main component. The other detected elements in all particles are: C, N, O and traces of steel and Inconel alloy constituents. The spherical droplet shown in Fig. 7(a) is not splashed and its composition is complex (see EDS spectrum in Fig. 7(b)). Besides light elements there are also heavy species: W, Mo, Ni, Cu and Fe. It gives a fairly strong indication that the origin of such particle(s) is not associated with melting and splashing of the limiter material. One may suggest that it is most probably a W-Mo or W-Ni particle formed earlier in another region of the machine and then transported, for instance, during a disruption. The deposition of other species (Be, C, N) occurred when the droplet was already residing on the mirror surface. This statement regarding the droplet composition and the sequence of events is justified by the detection of beryllium on the surface. The energy of Be($K_\alpha$) radiation is only 108 eV and would not have been detected if it was a Be droplet coated with high-Z species.

*3.2 Li-beam diagnostic mirrors*

Li-beam diagnostic mirrors were retrieved after the 2011-2012 and 2013-2014 campaigns. Images in Figure 8 show the appearance of those mirrors. In both cases, significant areas of their surfaces were damaged. The topography of the damaged area, as recorded by optical microscopy in Figure 9, clearly proves melting of the surface layer (Au coating and the

stainless steel substrate) by arcing. Arcing is a well-known erosion process in fusion devices [18-21]. The main conditions to form electric arcs are a sufficiently high potential and an electron-emission spot such as a small surface protrusion (for instance, a beryllium droplet). In the presence of magnetic fields, the cathode spot moves across the material in the direction perpendicular to the magnetic field. This effect is known as retrograde motion and it produces characteristic dendrite-like tracks, as those observed in the mirror [22].

Total and diffuse reflectivity in the visible and NIR range are presented in Figure 10. Total reflectivity decreased after plasma exposure from over 90% to about 60%. The values after plasma exposure resemble those characteristics for stainless steel. This suggests erosion of the gold layer and consequent mixing with stainless steel in the surface region. In the visible range, diffuse reflectivity increased from 2% to more than 15% as a result of surface roughening by arcing. In conclusion, optical properties of the mirror were significantly degraded.

The result of analysis with RBS for the mirror exposed during 2013-2014 is presented in Figure 11. Initially, there was a well-defined gold layer of 0.6 μm on top of a stainless steel substrate, while after exposure, the gold signal is reduced and overlaps with the stainless steel background. This indicates a reduction in the gold concentration by a factor of 2 (from 3.7 to 1.8 x $10^{18}$ $cm^{-2}$) and strong material mixing being a result of melting. In the damaged area, the concentrations of D and Be were up to 5 x $10^{17}$ $cm^{-2}$ and 10 x $10^{17}$ $cm^{-2}$, respectively. Deposition of impurities most probably formed hot spots for the initiation of electric arcs. In the non-damaged area, the concentrations of D and Be were much lower (about 1x$10^{16}$ $cm^{-2}$) because of the protection given by the crane rail placed in front of the periscope head (see Figure 1). Traces of C, N and O were also detected but they could not be quantified because of the surface roughness.

**4. Concluding remarks**

There are several important contributions of this work to the determination of plasma impact on the mirror performance and on material erosion and transport in the main vessel and in the divertor. Studies performed with a set of complementary material research techniques clearly show beryllium splashes and fine metal (W, Ni) droplets deposition on mirror surfaces in the main chamber. This has never been observed at earlier stages of FMT, neither in JET-C nor in JET-ILW. Mirrors in the divertor are coated with multi-layer deposits containing both W and

Be [23], thus proving transport of metals to shadowed regions. Mirrors, with their smooth surfaces can be considered as perfect deposition monitors. Using ToF-ERDA depth profiling, one can then "deconvolute" the operation history. It should be stressed that all specimens, both in the main chamber and in the divertor, contained nitrogen which was originally puffed only in the divertor region. Nitrogen levels are fairly constant over the entire operation period. Carbon content in mirrors is about 10 times lower in the second campaign with respect to the first campaign. Detection of only traces of carbon on surfaces provides a positive message regarding the stability of W coatings on tiles made of carbon fibre composites (CFC).

For the first time, surface analyses have been performed on a diagnostic mirror from JET. Part of the surface of the Li-beam diagnostic mirror was severely damaged by intense arcing. The gold coating layer and the stainless steel substrate of the mirror had been melted, changing completely its optical properties. The most probably reason for arc initiation is splashing of molten material from the surrounding limiters. This idea is supported by the significantly higher amount of deposits found in the area affected by arcing with respect to the non-damaged area, which was protected from impurity deposition by a crane rail structure placed in front of the periscope head. Based on these first studies of real diagnostic mirrors one concludes that components of other systems should be examined, especially to assess the state of the coatings.

**Acknowledgements**

This work has been carried out within the framework of the EUROfusion Consortium and has received funding from the Euratom research and training programme 2014-2018 under grant agreement No 633053. The views and opinions expressed herein do not necessarily reflect those of the European Commission. The work has been partly funded by the Swedish Research Council (VR) through contracts no. 621-2012-4148 and 2015-04844. We thank the staff of the Tandem Accelerator Laboratory at the Uppsala University for their help during the ion beam analysis measurements.

## 5. References


[1] A. E. Costley, et al., Fusion Eng. Des. 74 (2005) 109

[2] M. Rubel, et al., Rev. Sci. Instr. 77 (2006) 063501

[3] P. Wienhold, et al., J. Nucl. Mat. 337 (2005) 1116

[4] A. Litnovsky, et al., Fusion Eng. Des. 83 (2008) 79

[5] M. Lipa, et al., Fusion Eng. Des. 81 (2006) 221

[6] Y. Zhou, et al., Fusion Eng. Des. 81 (2006) 2823

[7] A. Garcia-Carrasco, et al., Nucl. Instr. Meth. B (2016) doi:10.1016/j.nimb.2016.02.065

[8] K. Ono et al., Phys. Scr. T138 (2009) 014065

[9] G.F. Matthews et al., Phys. Scr. T145 (2011) 014001

[10] M. Rubel, et al., J. Nucl. Mater. 390-391 (2009) 1066

[11] M. Rubel, et al., Phys. Scr. T145 (2011) 014070

[12] D. Ivanova, et al., Phys. Scr. T159 (2014) 014011

[13] M. Brix, et al., Rev. Sci. Instr. 81 (2010) 10D733

[14] M. Brix, et al., Rev. Sci. Instr. 83 (2012) 10D533

[15] P. Ström, et al., submitted to Rev. Sci. Instr.

[16] A. Baron-Wiechec, et al., Nucl. Fusion 55 (2015) 113033

[17] S. Brezinsek, et al., J. Nucl. Mater. 438 (2013) S303

[18] M Rubel et al., J. Nucl. Mater 307-311 (2002) 111

[19] M. Laux et al., J. Nucl. Mater 313-316 (2003) 62

[20] V. Rhode, et al., J. Nucl. Mat. 438 (2013) S800

[21] D. Rudakov, et al., J. Nucl. Mat. 438 (2013) S805

[22] B. Jüttner, et al., J. Phys. 33 (2000) 2025

[23] E. Fortuna et al., These Proceedings.

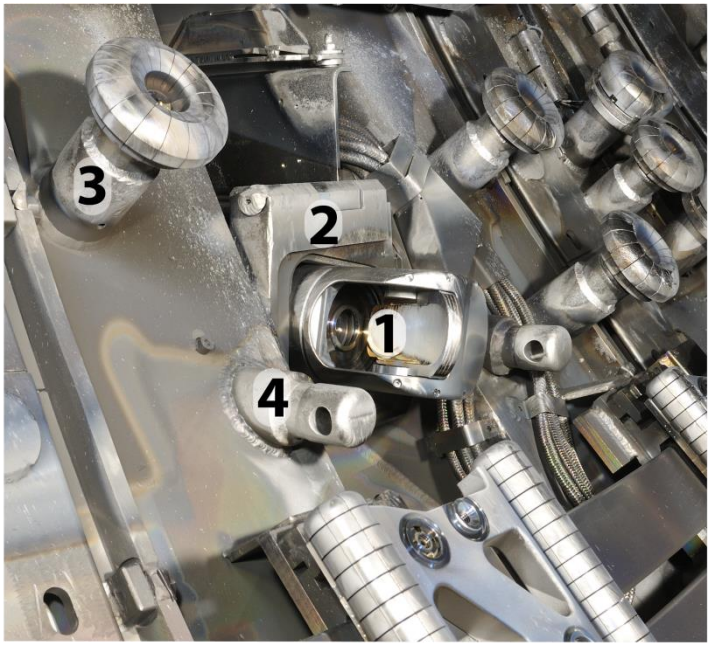


*Figure 1: Top of the JET vessel: 1) mirror, 2) periscope head, 3) castellated mushroom roof limiter, 4) crane rail.*

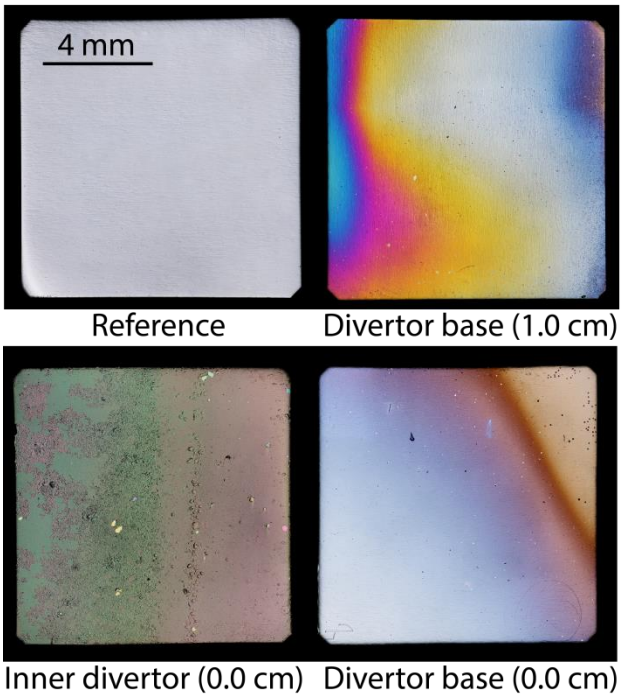


*Figure 2: Visual inspection of divertor mirrors after exposure to plasma.*

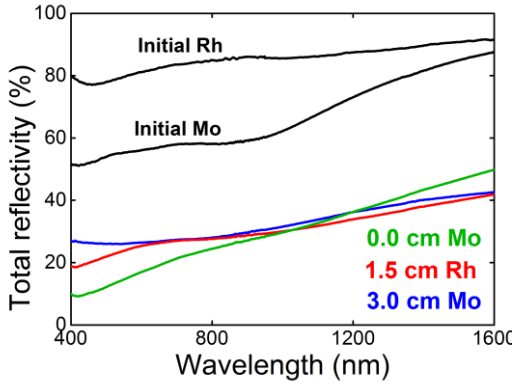


*Figure 3: Reflectivity of outer divertor mirrors before and after exposure to plasma. The distances 0.0, 1.5, 3.0 cm refer to the depth of the mirror in the channel of the carrier.*

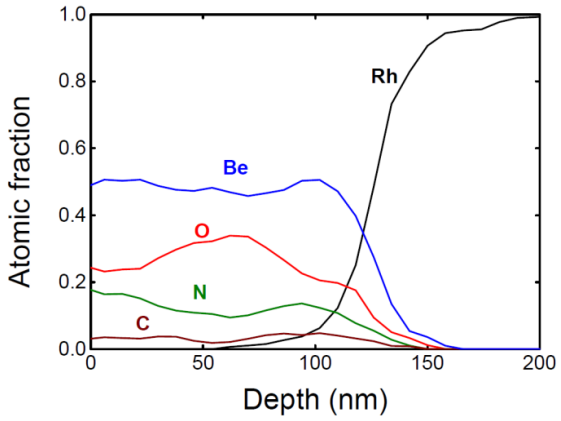


*Figure 4: Concentration depth profile of rhodium mirror located in the inner divertor, 1.5 cm deep into the channel of the carrier.*

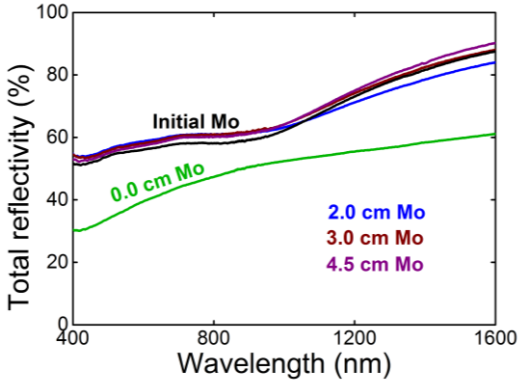


*Figure 5: Reflectivity of main chamber wall mirrors before and after exposure to plasma. The distances 0.0, 2.0, 3.0, 4.5 cm refer to the depth of the mirror in the channel of the carrier.*

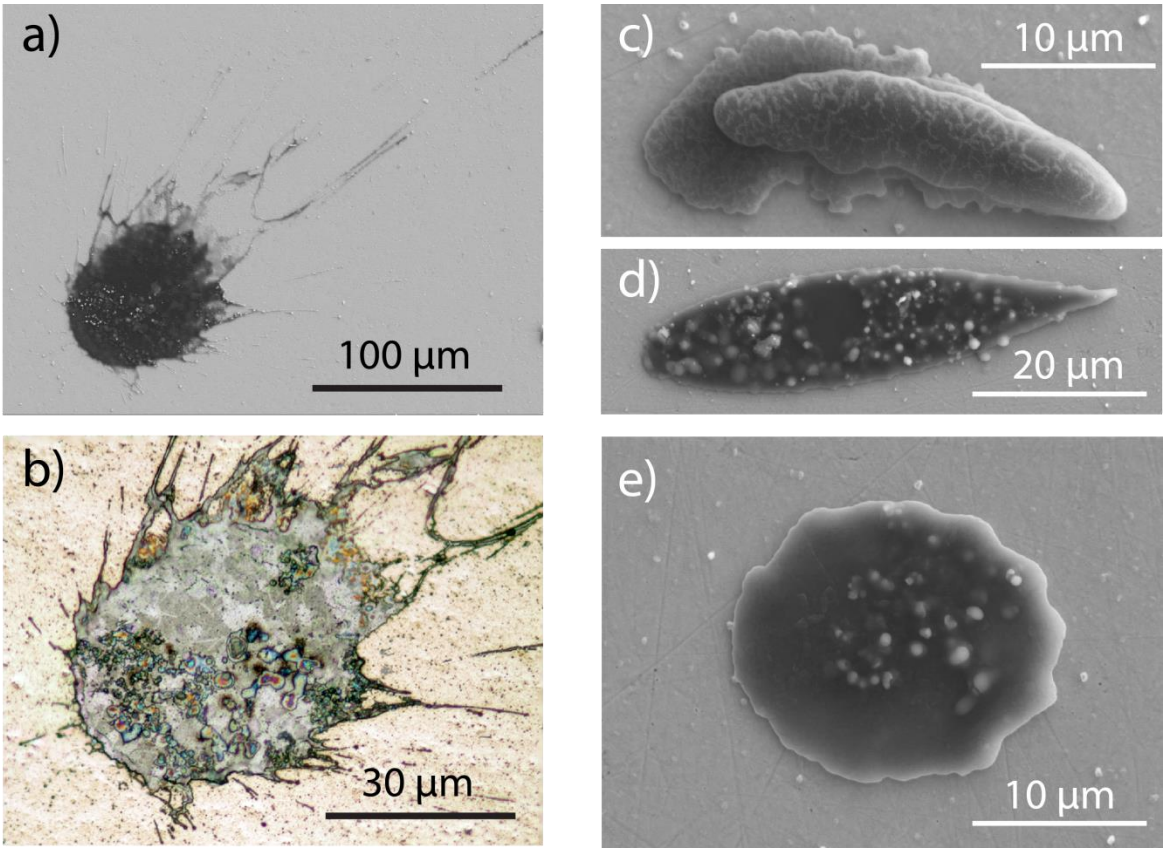


*Figure 6: Images of beryllium splashes on the surface of the mirror at position 0 cm. The splashes have elongated (a-d) or flat (e) shapes. Images (a) and (b) show the same particle under electron and optical microscopy respectively.*

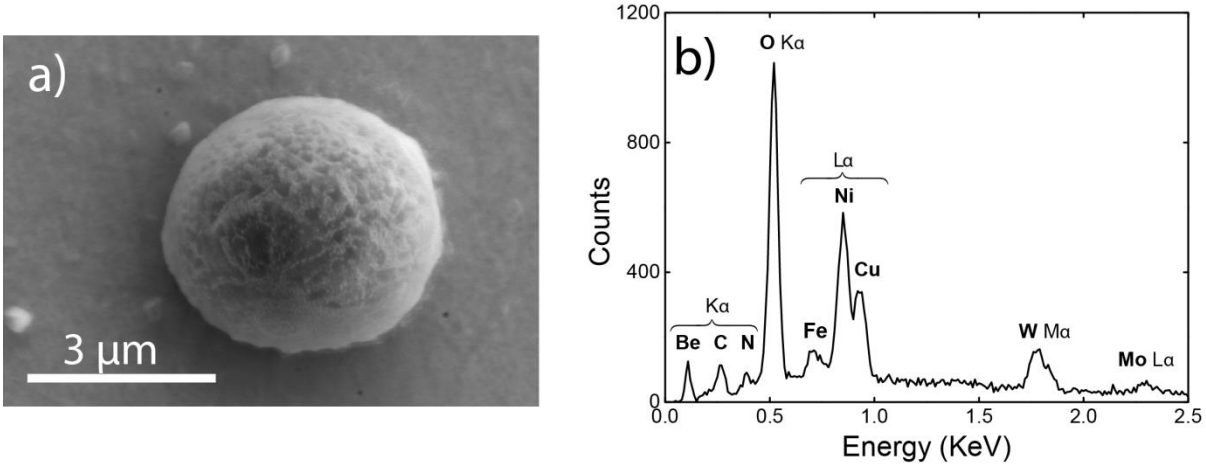


*Figure 7: (a) spherical droplet on the surface of the mirror at position 0 cm, (b) EDS spectrum of the spherical droplet.*

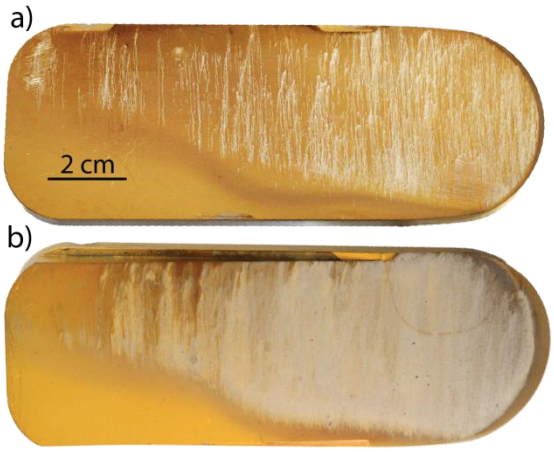


*Figure 8: Li-beam diagnostic mirrors after exposure in JET in a) 2011-2012 experimental campaign, b) 2013-2014 experimental campaign.*

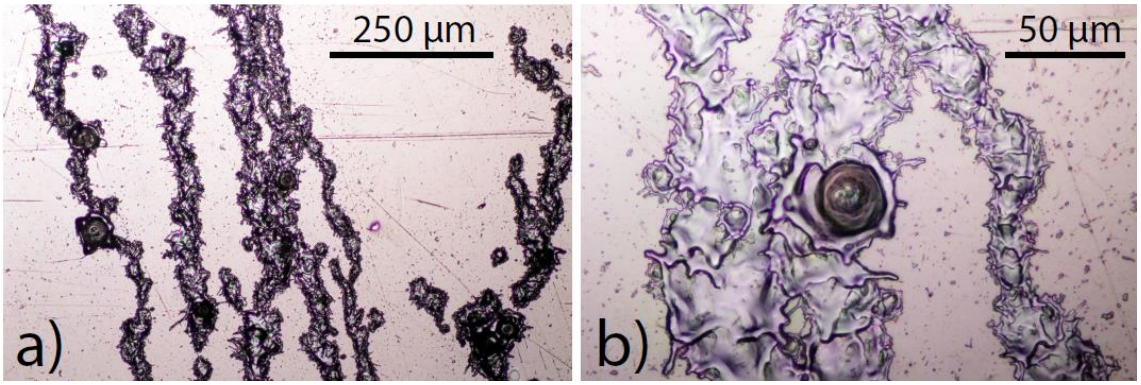


*Figure 9: Optical microscopy pictures of the surface of the Li-beam diagnostic mirror: a) arc traces along the mirror surface, b) detail of material melting produced by arcing.*

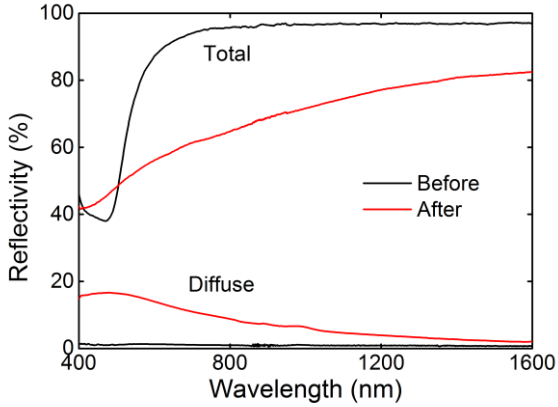


*Figure 10: Total and diffuse reflectivity of the Li-beam diagnostic mirror before and after exposure to plasma during the 2013–2014 campaign.*

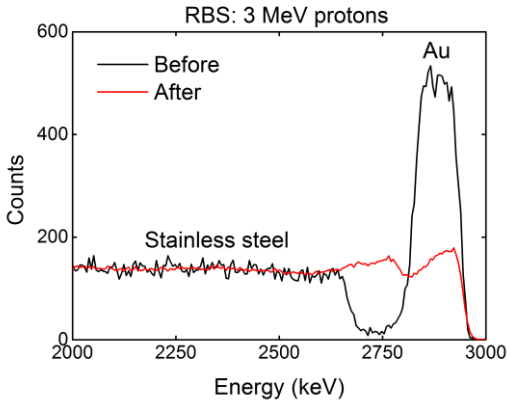


*Figure 11: RBS spectrum of the Li-beam diagnostic mirror before and after exposure to plasma during the 2013–2014 campaign.*

*Table 1: Composition of deposits of divertor mirrors. All numbers are in units of $10^{15}$ $cm^{-2}$.*

| | Inner | Base | Outer |
|---|---|---|---|
| D | 70 - 1391 | 69 - 245 | 23 - 680 |
| Be | 175 - 3602 | 353 - 670 | 325 - 4850 |
| C | 6 - 431 | 14 - 29 | 17 - 72 |
| N | 19 - 434 | 29 - 96 | 31 - 248 |
| O | 111 - 1950 | 304 - 652 | 226 - 1484 |
| W | 2 - 114 | 4 - 12 | 4 - 19 |

Table 2: *Composition of deposits of main chamber wall mirrors. The distances 0 cm and 1.5-4.5 cm indicate depth into the channel of the carrier. All numbers are in units of $10^{15}$ $cm^{-2}$.*

| | 0 cm | 1.5 - 4.5 cm |
|---|---|---|
| D | 390 | 3 - 20 |
| Be | 7300 | 0 - 5 |
| C | 30 | 20 - 30 |
| N | 94 | 0 - 5 |
| O | 1125 | 1 - 20 |
| W | 2 | 0 |